MASS ENERGY ABSORPTION COEFFICIENTS OF SELECTED BIOLOGICALLY EQUIVALENT MATERIALS

By

BASSAM ZUHDI OTHMAN SHAKHREET

Thesis submitted in fulfillments of the
requirements for the degree
of Master of Science

September 2001

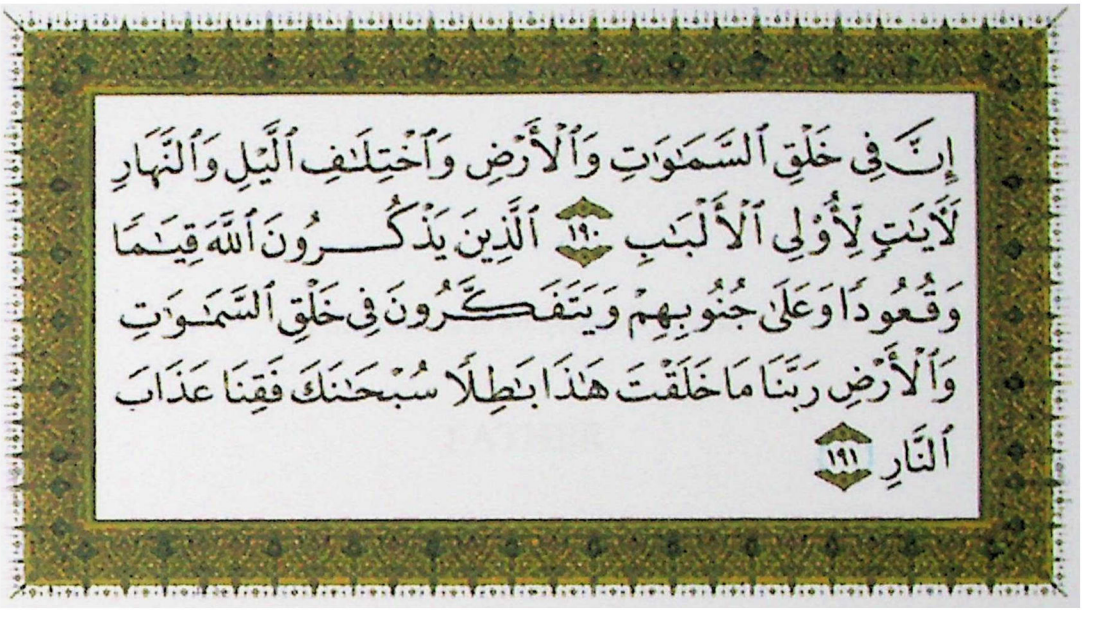
إِنَّ فِي خَلْقِ ٱلسَّمَٰوَٰتِ وَٱلْأَرْضِ وَٱخْتِلَٰفِ ٱلَّيْلِ وَٱلنَّهَارِ
لَءَايَٰتٍ لِّأُو۟لِى ٱلْأَلْبَٰبِ ﴿١٩٠﴾ ٱلَّذِينَ يَذْكُرُونَ ٱللَّهَ قِيَٰمًا
وَقُعُودًا وَعَلَىٰ جُنُوبِهِمْ وَيَتَفَكَّرُونَ فِى خَلْقِ ٱلسَّمَٰوَٰتِ
وَٱلْأَرْضِ رَبَّنَا مَا خَلَقْتَ هَٰذَا بَٰطِلًا سُبْحَٰنَكَ فَقِنَا عَذَابَ
ٱلنَّارِ ﴿١٩١﴾

Behold!

In the creation of Heavens and Earth, and in the alternation between night and daylight, there are signs for prudent persons who remember Allah while standing, sitting and (lying down) on their sides and contemplate the wonder of creation in the Heavens and the Earth with thought by saying: Our Lord! You have not created this in vain. Glory is to you. Give us salvation from the torment of fire.

DEDICATION

This Thesis is Dedicated To My

FATHER

Who Has Done His Best To Uplift Me, Without Whom I Would Not Have Been Able To Achieve This,

To My

MOTHER

For Her Love And Affection,

And To My

WIFE

For Her Support And Encouragement

ACKNOWLEDGEMENTS

The author's thanks and gratitude first goes to **ALLAH**, the Lord of mankind, jinn, and all that exists, who gave him the strength, inspiration and patience to continue this research. His thanks go also to many people who have contributed directly or indirectly in the completion of this research. Some of them deserve special mention.

The author expresses his sincere profound gratitude to his wonderful supervisor **Prof. Dr. Ahmad Shukri**, School of Physics, Universiti Sains Malaysia (USM), Malaysia whose valuable instructions, cooperation, constructive criticisms and exceptional role helped bring this thesis to reality. The author is indebted to him for imparting his wide experiences and knowledge in this field.

The author is also extremely grateful to **Prof. Dr. Abd Aziz Tajuddin**, his second supervisor, who guided him through out the thesis. He provided timely feedback and affirmative suggestions.

The author also owes a great deal of gratitude to **Prof. Dr. C. S. Chong** for the useful discussions, suggestions, contributions, and ideas.

Many thanks go also to **Universiti Sains Malaysia** for giving him the chance to continue his higher education. Thanks also to **Mr. Burhanudin Wahi** and **Mr. Azmi Omar** for their technical assistance.

There are many other people who assisted the author but have not been mentioned here. The author is grateful for their contributions.

Finally, the author is deeply in gratitude to his **parents, wife, sisters**, and **brother** for their prayers, patience, and support.

TABLE OF CONTENTS

LIST OF TABLES

LIST OF FIGURES

LIST OF APPENDICES

ABSTRAK

PEKALI SERAPAN TENAGA JISIM BAGI BAHAN SETARA BIOLOGI TERPILIH

Salah satu daripada kuantiti sinaran gama yang paling penting daripada segi penggunaan dosimetri sinaran dan fizik kesihatan ialah penyerapan jisim tenaga. Pengukuran pekali serapan jisim-tenaga, μ_{en}/ρ secara terus amat sukar dan lazimnya pengiraan teori menjadi pilihan. Dalam kajian ini kami telah menentukan μ_{en}/ρ dengan menggunakan suatu kaedah yang ringkas berdasarkan kaedah penghantaran sfera parapaksi menggunakan pengesan gama dengan respons berkadaran. Kesan-kesan tidak parapaksi dan kesan ketebalan sampel yang terhingga telah diambilkira menggunakan prosedur penentuluaran. Sisihan daripada ketidakkekadaran dan pembetulan lain telah ditunjukkan sebagai tidak signifikan.

Untuk foton 0.662 MeV, nilai μ_{en}/ρ yang diukur untuk lilin parafin menggunakan kaedah di atas dan didapati bernilai $(3.37 \pm 0.05) \times 10^{-3}$ m^2/kg. Nilai ini boleh dibandingkan dengan nilai yang diperolehi secara teori iaitu 3.35×10^{-3} m^2/kg yang diberikan oleh Hubbell dan Seltzer (1982). Nilai yang diukur untuk gipsum telah ditentukan sebagai $(2.96 \pm 0.01) \times 10^{-3}$ m^2/kg yang juga boleh dibandingkan dengan nilai yang diperolehi secara teori iaitu 2.99×10^{-3} m^2/kg yang diberikan oleh Hubbell dan Seltzer (1982).

Kajian yang terperinci dengan pengukuran menggunakan petala sfera dibandingkan dengan pengukuran menggunakan petala silinder telah juga dijalankan. Tujuan pengukuran tersebut adalah untuk menentukan kesetaraan di antara kedua-dua bentuk fantom. Selain daripada persoalan kepekaan pengukuran terhadap ketebalan petala-

petala, kajian juga mengkaji kebergantungan nilai yang diukur terhadap jarak pemisahan punca dan pengesan. Hasil yang diperolehi untuk kedua-dua bentuk fantom menunjukkan keserasian yang rapat daripada segi nilai-nilai μ_{en}/ρ yang diperolehi.

ABSTRACT

One of the most important gamma radiation quantities in respect of radiation dosimetry and health physics applications concerns is mass energy absorption. Direct measurements of the coefficient of mass-energy absorption, μ_{en}/ρ, are difficult and typically recourse is taken to theoretical computations. In this study we have determined μ_{en}/ρ using a simple and direct method based on paraxial sphere transmission using a proportional response gamma detector. The effects of nonparaxiality and of finite sample thickness have been accounted for, using extrapolation procedures. The deviation from nonproportionality and other corrections have been shown to be small.

For 0.662 MeV photons, the measured value of μ_{en}/ρ for paraffin wax has been determined using the above method as $(3.37 \pm 0.05) \times 10^{-3}$ m^2/kg. This compares favorably with the theoretically computed value of 3.35×10^{-3} m^2/kg given by Hubbell and Seltzer (1982). The measured value of (μ_{en}/ρ) for gypsum has been determined as $(2.96 \pm 0.01) \times 10^{-3}$ m^2/kg which also compares favorably with the theoretically computed value of 2.99×10^{-3} m^2/kg given by Hubbell and Seltzer (1982).

An extensive study where measurements using spherical shells were compared with those using cylindrical shells were also made, the intent being to determine the equivalence of these two phantom shapes. Besides the question of sensitivity of measurements to shell thickness, the investigation also examined the dependency of measured values on source to detector separation. Results obtained for the two shapes show close agreement with regards the values of μ_{en}/ρ obtained using either shape.

CHAPTER 1

INTRODUCTION

1.1 Introduction

When gamma ray photons pass through a medium, interactions between photons and matter can take place with the result that energy is transferred to the medium.

The initial step in the energy transfer involves the ejection of electrons from the atoms of the absorbing medium. These high-speed electrons transfer their energy by producing ionization and excitation of the atoms along their paths. If the absorbing medium consists of body tissues, sufficient energy may be deposited within the cells, destroying their reproductive capacity. However, most of the absorbed energy is converted into heat, producing no biological effect.

Most of the electrons set in motion by the photons will lose their energy by inelastic collisions (ionization and excitation) with atomic electrons of the material. A few, depending on the atomic number of the material, will lose energy by bremsstrahlung interactions with the nuclei. The bremsstrahlung energy is radiated out of the local volume as x-rays and is not included in the calculation of locally absorbed energy.

There are three primary interactions by which energy is absorbed. These interactions result in either complete absorption of the gamma photon, or the scattering of the photon at a different energy and direction, or the complete disappearance of the

photon and the creation of matter and antimatter particles instead. These are commonly known as the photoelectric effect, Compton scattering, and pair production respectively.

The effects of gamma rays on irradiated media are largely indirect, i.e., they occur via electrons (or positrons) which are set in motion as a result of gamma ray interactions with matter, and then dissipate their energy as they are brought to rest. The relation between electron (or positron) energy deposition in a medium and the various physical, chemical, and biological effects is complicated and, in most cases, not well understood. However, it is commonly assumed that the amount of energy absorbed per unit mass of the medium (absorbed dose) is a significant parameter which provides a basis for discussing radiation effects.

The mass attenuation coefficient, μ/ρ, and the mass energy absorption coefficient, μ_{en}/ρ, are basic quantities used in calculations of the penetration and the energy deposition by photons (x-ray, γ-ray, bremsstrahlung) in biological, shielding and other materials (ICRU Report 33, 1980).

The *mass attenuation coefficient*, μ/ρ, is a measure of the average number of interactions between incident photons and matter that occur in a given mass-per-unit-area thickness of material encountered. The *mass energy absorption coefficient*, μ_{en}/ρ, on the other hand, is a measure of the average fractional amount of incident photon energy transferred to kinetic energy of charged particles set in motion as a result of these interactions.

This imparted charged-particle kinetic energy, in turn, is a more or less valid approximation, depending on the absorber, absorber dimensions, photon energy and other factors, to the amount of energy made available for the production of chemical,

biological, and other effects associated with exposure to ionizing radiation (Berger, 1961). The mass energy absorption coefficient has thus assumed an essential role in estimating absorbed dose, whether from a calculated X-ray intensity or from measurements with an ionization chamber.

The coefficient of photon-interaction most appropriate to radiation dosimetry is that of *mass energy absorption coefficient*, μ_{en}/ρ, which refers to the amount of energy dissipated by the secondary electrons set in motion as a result of interactions between the incident photons and matter, where ρ is an absorber density. Under certain conditions, the energy dissipated by the electrons in the given volume can be equated to the energy absorbed in that volume.

The mass energy absorption coefficient, μ_{en}/ρ, is an important quantity in radiotherapy since it allows the evaluation of energy absorbed in the tissues, a quantity of interest in predicting the biological effects of radiations.

For most interactions involving soft tissues or other low Z materials in which electrons lose energy almost entirely by ionization collisions, the bremsstrahlung component is negligible. Thus $\mu_{en}/\rho = \mu_{tr}/\rho$ under those conditions, where μ_{tr}/ρ is another coefficient which allows only for the escape of Compton-scattered, fluorescence and annihilation photons (ICRU Rep. 10b, 1964). These coefficients can differ appreciably when the kinetic energies of the secondary particles are high and the material traversed has a high atomic number.

Direct accurate measurements of μ_{en}/ρ are difficult. Evaluation by calorimetric measurements, yielding temperature changes of the order of a millikelvin or less are typically limited to standardizing laboratories. However, one other possibility for direct

evaluation of μ_{en}/ρ is through energy-proportional detection for unmodified and modified photon-spectra, the measured transmission factors being directly related to energy absorption. Earlier measurements were exclusively made using spherical shells of low atomic number media (Bradley *et. al*, 1989). A particular problem relates to the shape and thickness of an absorber; symmetry indicates use of spherical absorbers, while physical constraints further indicate use of thin shells (generally being of thickness less than one mean-free-path "m.f.p."). Greater utility of the method would seem to suggest formulation of more-easily-fabricated shapes offering equivalence of response.

Many other investigators have also studied energy absorption coefficient of different energies and materials in order to get agreement between measured and theoretical values.

Cunningham *et. al* (1986) used the Monte Carlo computer code "electron gamma shower" (EGS) to determine photon spectra in a water phantom. They studied the dependency of mass energy absorption coefficient ratios on beam size and depth in a phantom.

Linear absorption and mass absorption coefficients of 0.123 MeV gamma radiation from ^{57}Co by dilute solutions of ($MgCl_2.6H_2O$) salt were studied by Teli *et. al* (1994a) for varying concentrations. This study explored the validity of the expected exponential absorption law for gamma radiation in solutions and also provided an alternative method for the direct determination of absorption and mass attenuation coefficients of soluble salts in solid form without obtaining them in a pure crystalline form.

The sphere transmission method was also employed by Bhandal *et. al* (1994) for the direct measurement of the mass energy absorption coefficients at 0.662 and 1.115 MeV of some fatty acids. Excellent agreement was obtained between the measured and theoretical values.

Teli and Chaudhari (1996) have studied the concentration dependence of the attenuation of gamma radiation of various energies by KCl solutions of different concentrations. The direct measurement of linear attenuation and mass absorption coefficients of dilute solutions of salts was also applied by them to the attenuation of 0.662 MeV gamma rays from ^{137}Cs in dilute NH_4Cl solution.

Singh *et. al* (1996a) used a sphere transmission method and employed it for the direct measurement of the mass energy absorption coefficients at 0.662 MeV of some compounds such as $FeSO_4$, TiO_2, $C_4H_{16}ClNO_3$, EDTA (Tris Buffer), Boric acid, and Diethylene triamine acetic acid. Excellent agreement was obtained between the measured and theoretical values.

1.3 Scope and Objectives

The main objective of the work is to carry out a thorough investigation of the paraxial sphere transmission method using a proportional response gamma detector in the determination of μ_{en}/ρ. The scope of work involves measurements of spherical and cylindrical paraffin wax ($C_{16}H_{34}$) and gypsum ($CaSO_4.2H_2O$) for the photon-energy 0.662 MeV.

The specific objectives of the present study reported in this thesis are:

a. To determine μ_{en}/ρ for paraffin wax and gypsum.

b. To compare the response of spherical absorbers with that of the cylindrical absorbers.

c. To look at the question of sensitivity of measurements to shell thickness.

d. To examine the dependency of measured values on source to detector separation, where the method is only strictly valid for point sources and point detectors.

CHAPTER 2

INTERACTIONS OF IONIZING RADIATION

2.1 Introduction

The process by which a neutral atom acquires a positive or negative charge is known as ionization. Removal of an orbital electron leaves the atom positively charged, resulting in an ion pair. The stripped electron, in this case, is the negative ion and the residual atom is the positive ion. In some cases, a neutral atom may acquire an electron and the negatively charged atom then becomes the negative ion.

Charged particles such as electrons and α particles are known as directly ionizing radiation provided they have sufficient kinetic energy to produce ionization by collision as they penetrate matter. The energy of the incident particle is lost in a large number of small decrements along the ionization track in the medium, which an occasional interaction in which the ejected electron receives sufficient energy to produce a secondary track of its own, known as a δ ray. If, on the other hand, the energy lost by the incident particle is not sufficient to eject an electron from the atom but is used to raise the electrons to higher energy levels, the process is termed excitation.

Uncharged particles such as neutrons and photons are indirectly ionizing radiation since they liberate ionizing particles when they interact with matter.

Ionizing photons interact with the atoms of a material or absorber to produce high-speed electrons by three major processes: photoelectric effect, Compton effect, and pair production.

2.2 Gamma-ray Spectroscopy

Figure 2.1 shows the special case where a gamma source is being counted by a lead-shielded NaI (T*l*) detector.

The photoelectric effect gives a well-defined peak in the measured spectrum. Gamma rays enter the NaI (T*l*) crystal and interact primarily with the bound K or L shell electrons from the iodine in the crystal. Essentially, the gamma gives all of its energy to the bound electron and knocks it out of the atom with an energy E_e given by:

$$E_e = h\nu + \Phi \qquad (2.1)$$

where Φ is the binding energy of the electron. Since Φ is only 33 keV for the iodine K shell, one can see that the recoiling electron has most of the energy of the incident gamma ray which is usually of the order of 1 MeV or more. As this recoiling electron goes through the NaI (T*l*) crystal, it loses its energy by ionization, excitation, and the production of thermal energy. Some fixed fraction of the electron energy will be converted to light photons, which then impinge on the photocathode of the photomultiplier tube (as shown in figure 2.1).

These photons will produce photoelectrons from the photocathode surface (only one is shown in the Figure). These photoelectrons are attracted to the first dynode of the phototube by a positive voltage on it provided by the voltage divider resistor string attached to the photocathode of the phototube.

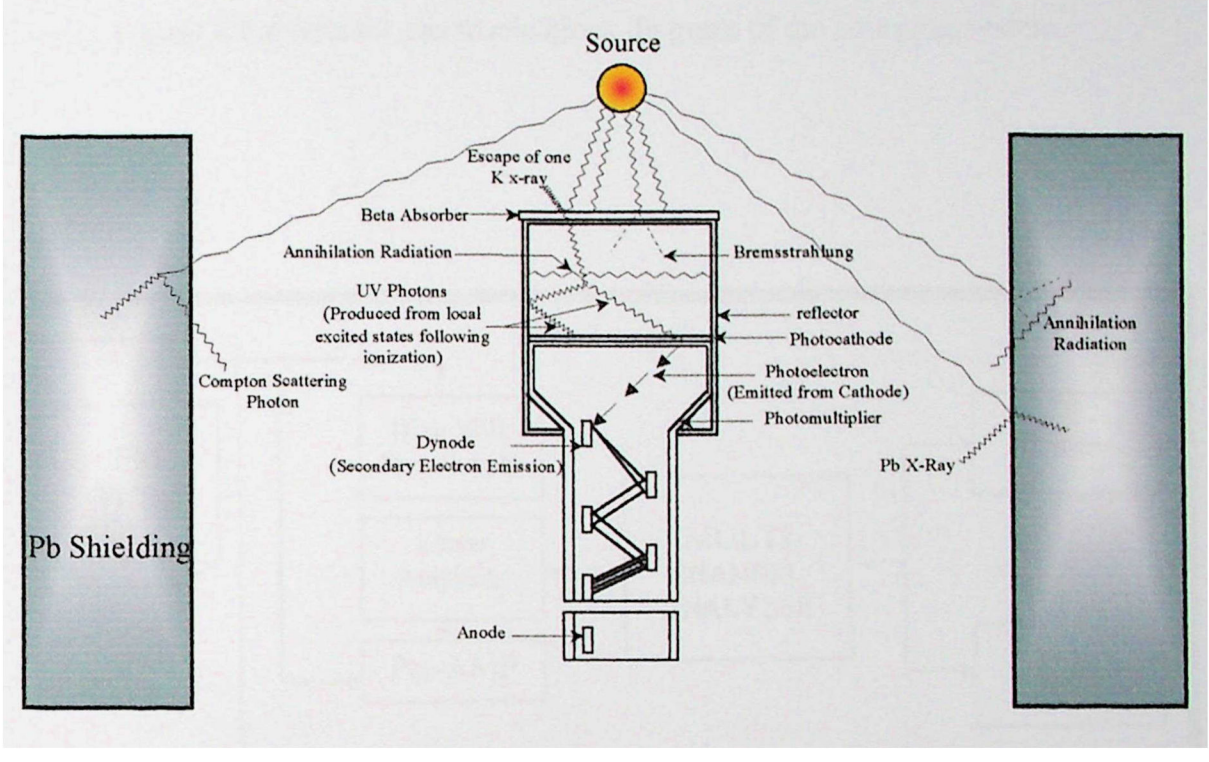

Figure 2.1 *A diagram showing the scintillation detector with various types of interactions.*

Secondary electrons emitted by the first dynode are attracted to the second dynode and so forth. The final avalanche of electrons arrives at the anode and produces an electrical pulse that is proportional to the energy of the incident gamma photon. These pulses are then amplified and fed to the channels of a multichannel analyzer system for analysis. Figure 2.2 shows the electronic block diagram of the counting system.

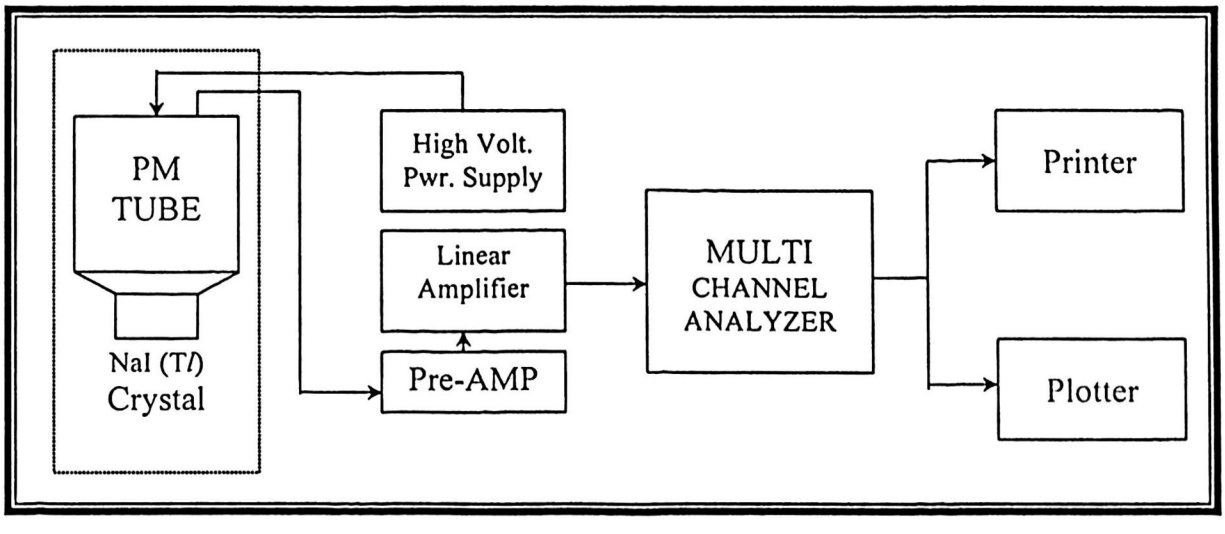

Figure 2.2 A *block diagram showing the components of a typical gamma spectroscopy system.*

A typical pulse height spectrum of ^{137}Cs that is provided by a multichannel analyzer system is shown in Figure 2.3. The photopeak is clearly seen at channel 1408 of the 4090-channel spectrum. The position of this photopeak channel is proportional to the gamma ray energy of ^{137}Cs (0.662 MeV). Since this system is linear, a gamma source with energy 1.32 MeV would occur in channel 2809. In addition, a small backscatter peak can be observed at energy of 0.184 MeV. This backscatter peak comes

from the fact that by analyzing the energy of a ^{137}Cs photon that is scattered by Compton interaction from the lead shield and then the scattered photon enters the NaI (T*l*) detector and is absorbed by the photoelectric effect. Since most of these photons scatter at about 180°, they are called backscattered photons. From the kinematic analysis of the Compton interaction, the scattered energy of these backscattered photons is 0.184 MeV.

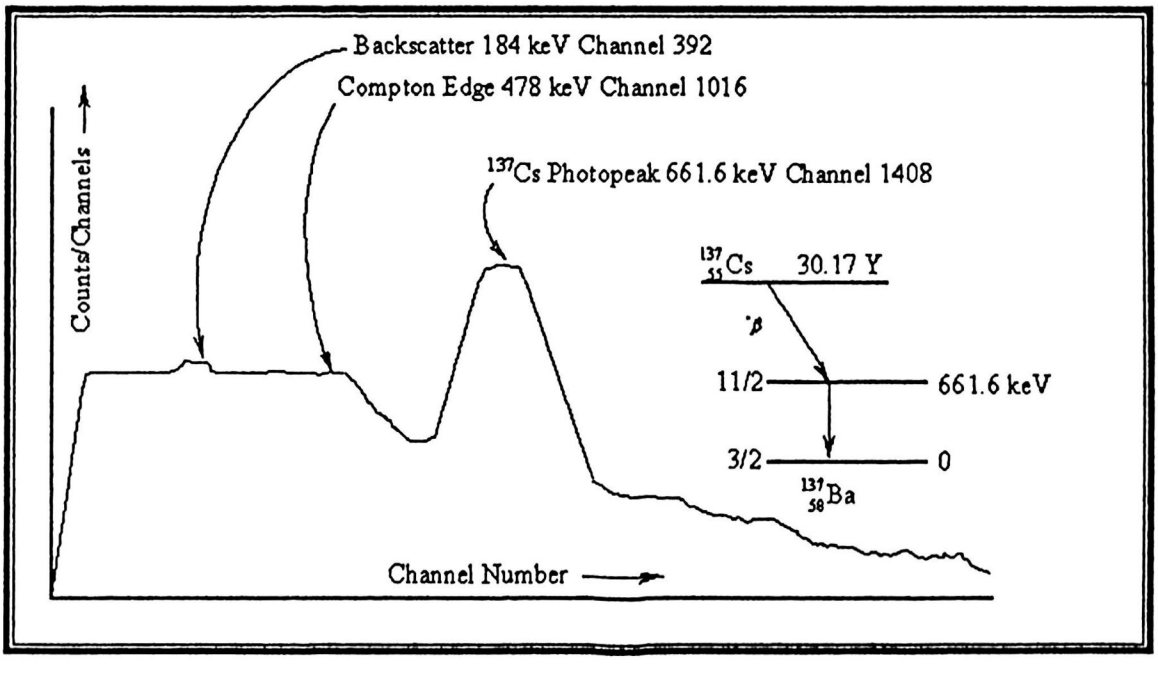

Figure 2.3 A *typical scintillation spectrum of* ^{137}Cs *showing the important interactions.*

Backscatter will also occur from the table, detector housing, detector supports, etc. Most of these backscattered photons come from the lead shield that may surround the detector. This shield, however, is necessary to reduce the room background radiation

from entering the detector. This background is by far the larger problem than the backscatter peak by the lead shield. It is easy to calculate the position of the backscatter peak by using the following equation:

$$E_\gamma^{'} = E_\gamma / [1 + (1 - \cos\theta)\, E_\gamma / m_o c^2] \qquad (2.2)$$

where $E_\gamma^{'}$ is the energy of scattered photon, E_γ is the incident photon energy and m_o is the rest mass of an electron or positron.

Since $m_o c^2 = 0.511$ MeV, and $\theta = 180^\circ$, then

$$E_\gamma^{'} = E_\gamma / (1 + 3.91\, E_\gamma) \qquad (2.3)$$

The Compton interaction is a purely kinematic collision between the incident gamma photon and an electron in the crystal that is either free or loosely bound. The incident gamma ray has energy $E = h\nu$ that is shared between the Compton scattered photon and the recoiling electron. The photon will be scattered at a lower energy $h\nu'$ while the recoil electron will have energy of T_e-. Since the total energy is conserved in the interaction, one can write:

$$h\nu = h\nu' + T_e\text{-} \qquad (2.4)$$

Since the linear momentum is also conserved in this interaction (see Figure 2.4), then from the conservation of momentum along the *x* direction, and along the *y* direction, respectively, we get:

$$h\nu/c = h\nu' \cos(\theta)/c + P \cos(\theta) \qquad (2.5)$$

$$0 = h\nu' \sin(\theta)/c - P \sin(\theta) \qquad (2.6)$$

where P is the linear momentum of the recoil electron. From these equations, one can obtain the energy of the scattered photon in terms of its initial energy, hν, and the scattered angle, θ. This energy is found to be:

$$h\nu' = h\nu / [1 + (1 - \cos(\theta)h\nu / m_o c^2] \qquad (2.7)$$

The kinetic energy of the Compton electron can be written as:

$$T_{e^-} = h\nu - h\nu' \qquad (2.8)$$

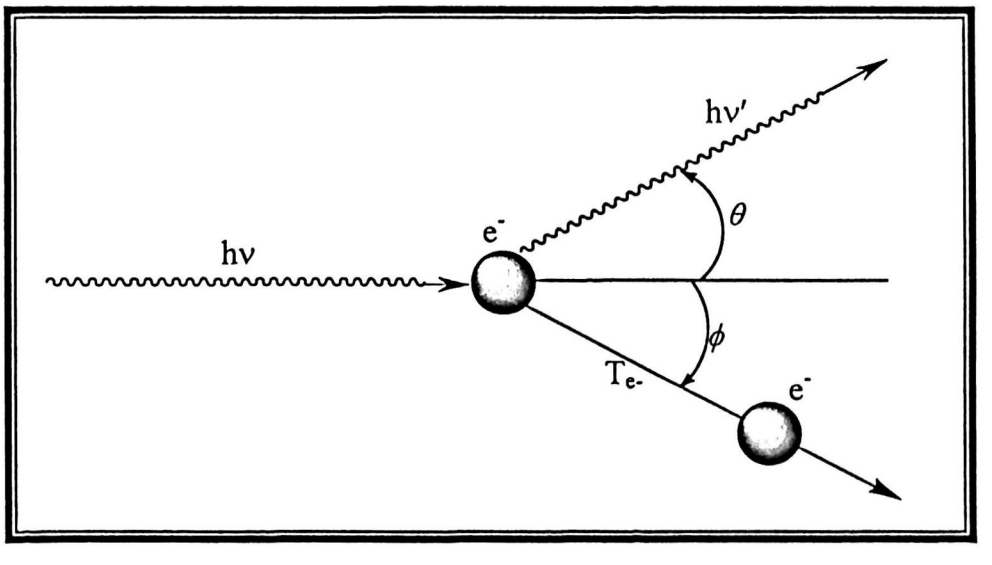

Figure 2.4 *The kinematics of Compton interaction.*

An examination of the last two equations indicates that the scattered photon may recoil at any direction with respect to the incident gamma photon. The Compton electron, however, can only be scattered in the forward direction. Table 2.1 shows the

expected energies of the scattered photon and Compton electron. These values were found by using the last two equations, and substituting different values of scattering angle θ and incident gamma energies.

Table 2.1 *The expected energies of the scattered photon and Compton electron.*

θ (degree)	hν = 0.662 MeV	
	hν′	T_e-
0	0.662	0
30	0.564	0.098
60	0.402	0.260
90	0.288	0.374
120	0.225	0.437
150	0.194	0.468
180	0.184	0.478

From the fact that all angles for the scattered photon are about equally probable, the recoiling electron energies T_e are equally probable from zero to a maximum value. The maximum recoil electron energy in the case of the ^{137}Cs-gamma photon corresponds to 0.478 MeV that corresponds to the Compton edge in Figure 2.3.

For incident gamma photons that have energies in excess of 1.02 MeV, the most probable interaction with the NaI (T*l*) crystal is pair production (see Figure 2.5). In this process the photon, near the nucleus of an atom, gives up all of its energy and produces an electron and a positron pair.

The minimum energy needed for pair production is given by $E = 2m_oc^2$. Since the rest mass of an electron is equivalent to 0.511 MeV, the photon must have energy greater than 1.02 MeV for the pair production to be detected.

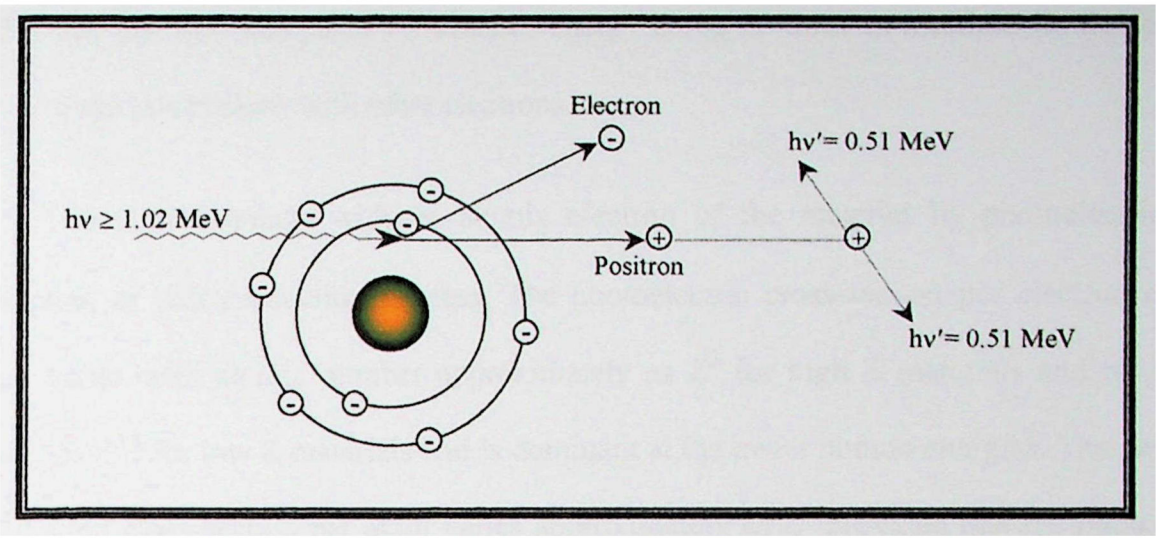

Figure 2.5 *A diagram showing the formation of an electron-positron pair.*

When this process occurs, energy of the photon beyond 1.02 MeV is given to the electron-positron pair as kinetic energy, and to the nucleus to conserve momentum. In a few nanoseconds, the positron interacts with an electron in the detector in a process called pair annihilation (destruction), whereby two gamma photons with energy of 0.511 MeV (or more) appear in nearly opposite directions.

Since this process does not occur when the gamma photon has energy less than 1.02 MeV, it is only significant for gamma of higher energies. This interaction is also proportional to Z^2 of the absorber. Therefore, pair production predominates for substances with high Z and for gamma energies above 5 MeV.

2.3 Gamma-ray Interaction With Matter

For gamma-ray dosimetry it is important to know that a gamma ray "photon" deposits its energy in matter via a two-step sequence:

a.) The γ-ray transfers its energy to an atomic electron.

b.) The electron dissipates the kinetics energy along its track in multiple Coulomb-force interactions with other electrons.

The γ-ray interacts with an atomic electron of the material by photoelectric, Compton, or pair-production process. The photoelectric cross-section per electron or gram varies with atomic number approximately as Z^3 for high Z materials and more nearly as $Z^{3.8}$ for low Z materials and is dominant at the lower photon energies. The pair production cross-section per atom varies approximately as Z^2 provided that the photon energy is higher or at least equals 1.02 MeV for the process to occur. The Compton process is much more important than either the photoelectric or pair production process for photons in the range 100 keV to 10 MeV. For low-Z media, the region of Compton-effect dominance is very broad and narrows with increasing Z.

In the current study, the low Z media –Paraffin Wax and Gypsum–, and the medium energy range of ^{137}Cs source lies within the range where Compton effect dominates.

CHAPTER 3

MASS ENERGY ABSORPTION COEFFICIENT μ_{en}/ρ

3.1 Introduction

To help us with our discussion of mass energy absorption coefficient μ_{en}/ρ we will first start by introducing the concept of *exponential attenuation* at this point. This concept is relevant primarily to uncharged ionizing radiations (i.e., photons and neutrons), which lose their energy in relatively few large interactions, rather than charged particles, which typically undergo many small collisions, losing their kinetic energy gradually.

An individual uncharged particle (photon or neutron) has a significant probability of passing straight through a thick layer of matter without losing any energy, while a charged particle must always lose some or all of its energy. An uncharged particle has no limiting "range" through matter, beyond which it cannot go; charged particles all encounter such a range limit as they run out of kinetic energy. For comparable energies, uncharged particles penetrate much farther through matter, on the average, than charged particles, although this difference gradually decreases at energies above 1 MeV.

3.2 Absorption of Energy

When a beam of photons passes into an absorbing medium such as body tissues, some of the energy carried by the beam is transferred to the medium where it may

produce biological damage. The energy deposited per unit mass of the medium is known as the absorbed dose and is a very useful quantity for the prediction of biological effects.

As it is illustrated in Figure 3.1, the initial step in the process usually involves the collision between a photon and some electrons in the body, resulting in the scattering of some radiation and the setting in motion of a high speed electron (represented by A in Figure 3.1). In traveling through tissue, the high-speed electron produces a track along which ionizations occur, excitation of atom takes place, and molecular bonds are broken (represented by B in Figure 3.1). All of these result in biological damage. Most of the energy however is converted into heat, producing no biological effect. Some of the high-speed electrons may suffer a collision with a nucleus and produce bremsstrahlung. This bremsstrahlung, as well as the scattered radiation, can undergo interactions in the same way as the original photon. Usually some 30 interactions are required before all the energy of the photon is converted into electronic motion.

3.3 Simple Exponential Attenuation

Assume that a slab of homogeneous material of thickness X is placed in the path of a monoenergetic parallel beam consisting of a very large number N_0 of photons incident perpendicularly on that slab as shown in Figure 3.2.

In an ideal case, it is assumed that each particle either is completely absorbed in a single interaction, producing no secondary radiation, or passes straight through the entire plate unchanged in energy or direction.

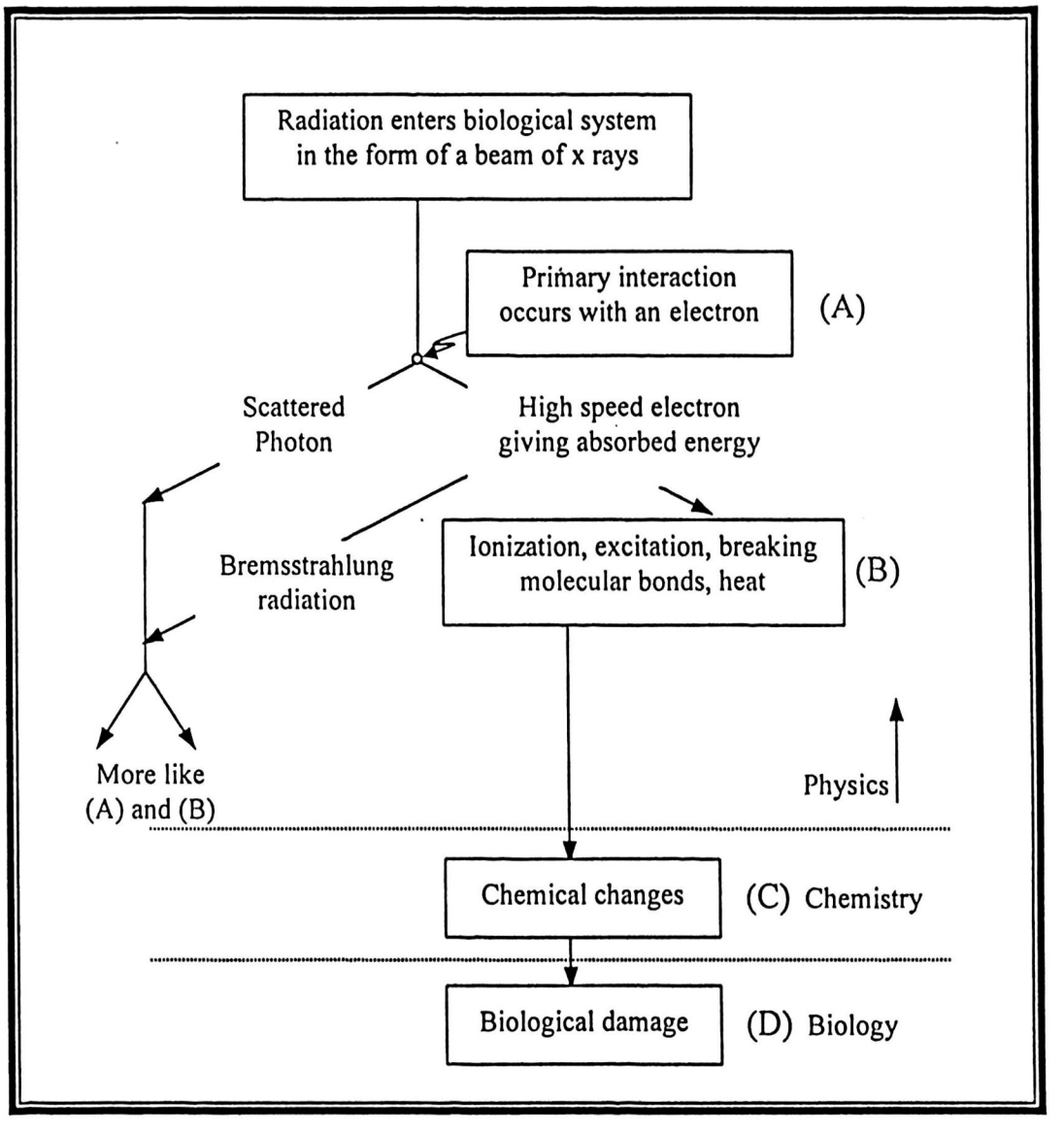

Figure 3.1 *Schematic diagram illustrating the absorption of energy from radiation resulting in biological damage (Johns and Cunningham, 1983).*

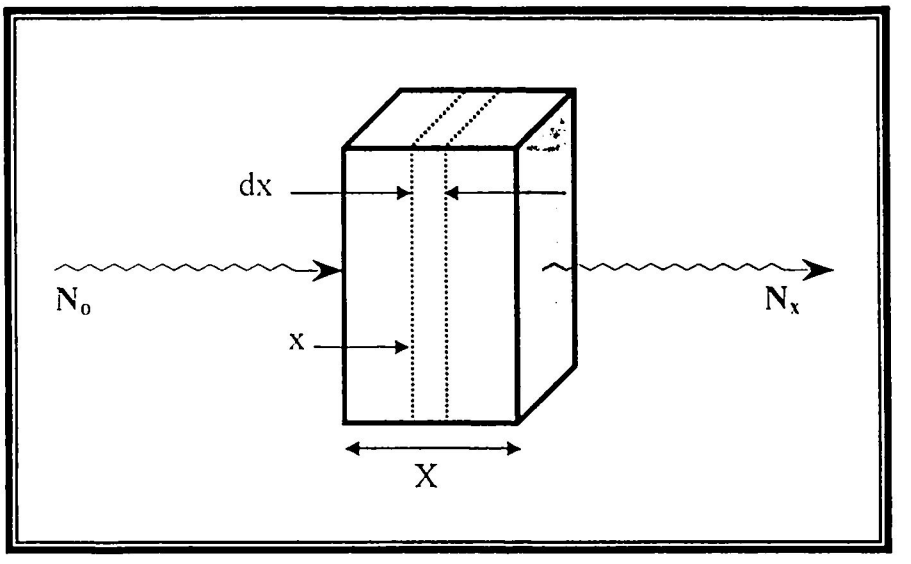

Figure 3.2 *Simple exponential attenuation (Attix, 1986).*

Suppose (μx) is the probability that an individual particle interacts in a unit thickness of material traversed, then the probability that it will interact in an infinitesimal thickness dx is μ dx. If N particles are incident upon dx, the change dN in the number N due to absorption is given by:

$$dN = -\mu N dx \qquad (3.1)$$

where μ is typically given in a unit of cm^{-1} or m^{-1}, and dx is correspondingly in cm or m.

The fractional change in N due to absorption of particles in dx is just:

$$\frac{dN}{N} = -\mu dx \qquad (3.2)$$

Integrating over the depth x from 0 to X, and corresponding particle populations from N_o to N_x, gives:

$$\int_{N_o}^{N_x} \frac{dN}{N} = -\int_{x=0}^{X} \mu dx$$

$$\frac{N_x}{N_o} = \exp(-\mu X) \qquad (3.3)$$

where N_x is the number transmitted by any thickness X, N_o is the number incident, e is the base of the natural logarithms with the value 2.718.

This is the law of exponential attenuation, which applies either for the ideal case described above (simple absorption, no scattering or secondary radiation), or where scattered and secondary particles may be produced but are not counted in N_x.

The above equation can also be written in terms of intensity (I):

$$dI = -\mu I\, dx \quad \Rightarrow \quad dI/I = -\mu\, dx$$

$$I(x) = I_o \exp(-\mu\, dx) \qquad (3.4)$$

The quantity μ is called the *linear attenuation coefficient*, or simply the attenuation coefficient. When it is divided by the density ρ of the attenuating medium, the mass attenuation coefficient μ/ρ (cm^2/g or m^2/kg) is obtained. This quantity will be discussed in Section 3.5.

The quantity $1/\mu$ (cm or m) is known the mean free path "m.f.p." or relaxation length of the primary particles. It is the average distance a single particle travels through a given attenuating medium before interacting. It is also the depth to which a fraction 1/e ($\cong$37%) of a large homogeneous population of particles in a beam can penetrate. Its value can be obtained from :

$$\lambda = \frac{\int_0^\infty x\, e^{-\mu x}\, dx}{\int_0^\infty e^{-\mu x}\, dx} = \frac{1}{\mu}$$

A distance of three mean free paths, $3/\mu$, reduces the primary beam intensity to 5%, $5/\mu$ to < 1%; and $7/\mu$ to < 0.1%. Typical values of λ (mean free path) range from a few mm to tens of cm in solids for common gamma-ray energies.

3.4 Narrow-beam and Broad-beam Attenuation of Uncharged Radiation

3.4.1 Narrow-Beam attenuation

There are two general methods of achieving narrow-beam attenuation:

- *Discrimination* against all scattered and secondary particles that reach the detector, on the basis of particle energy, penetrating ability, direction, coincidence, anticoincidence, time of arrival (for neutrons), etc.
- *Narrow-beam geometry*, which prevents any scattered or secondary particles from reaching the detector.

Figure 3.3 illustrates the essential features of narrow-beam geometry. The detector is placed far enough from the attenuating layers so that any particle S that is deflected in an interaction will miss the detector. The beam is collimated to be just large enough to cover the detector uniformly, thereby minimizing the number of scattered or secondary particles generated in the attenuator. The radiation beam source is located a large distance from the attenuator so that the particles are almost perpendicularly incident. Moreover, the intensity of the primary beam at the detector

will then be nearly independent of distance from the attenuator, while the intensity of the scattered and secondary particles will decrease as the inverse square of that distance. Thus the relative strength of the primary beam increases with detector distance, allowing reduction of the nonprimary radiation fraction to a negligible level at the detector.

The shield is assumed to stop all radiation incident upon it except that passing through its aperture. If it allows any leakage, it may be necessary to put a supplementary shield around the detector, as shown in Figure 3.3, that allows entry of radiation only at angles $\theta \cong 0^{\circ}$. Lead is the usual shielding material for x- or γ-rays, especially where space is limited. Narrow-beam geometry is sometimes referred to as "good" geometry (Evans, 1955).

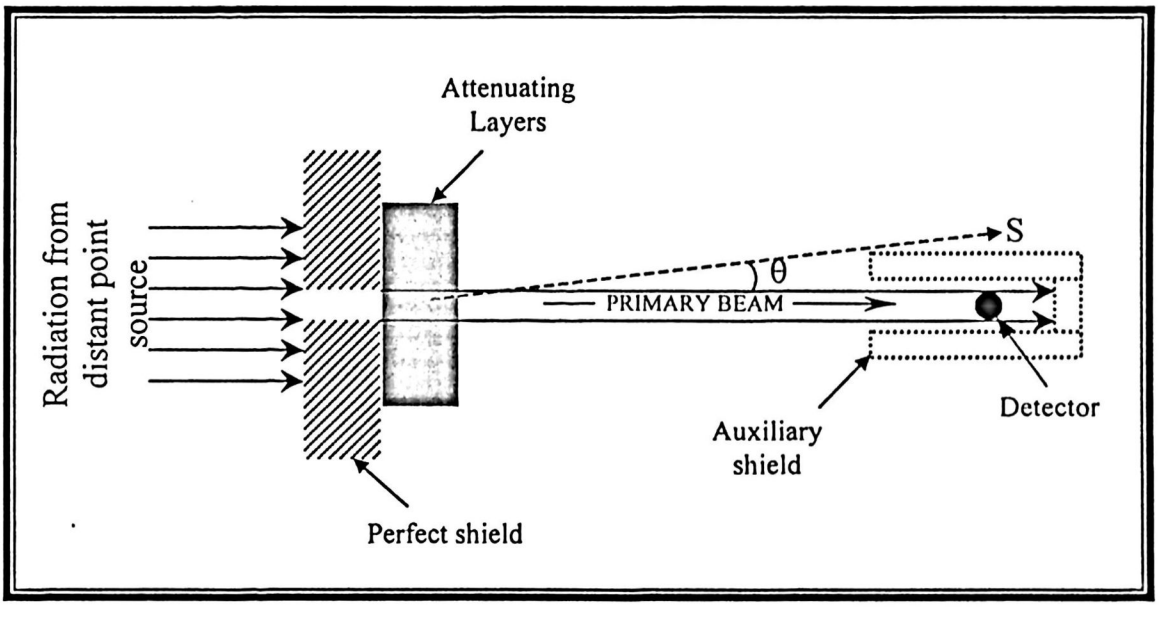

Figure 3.3 *Narrow-beam geometry. The diameter of the primary photon or neutron beam is made just large enough to cover the detector uniformly. The detector is placed at a large enough distance from the attenuator that the number of scattered or secondary particles (S) that reach the detector is negligible in comparison with the number of primary rays (Attix, 1986).*

3.4.2 Broad-Beam Attenuation

Any attenuation geometry other than narrow beam geometry – i.e., in which at least some nonprimary rays reach the detector – is called *broad beam geometry.*

It will be found useful to establish such a concept for comparison with actual cases. It may be defined as follows:

> "In – ideal broad - beam geometry every scattered or secondary uncharged particle strikes the detector, but only if generated in the attenuator by a primary particle on its way to the detector, or by a secondary charged particle resulting from such a primary." (Attix, 1986).

This requires that the attenuator be thin enough to allow the escape of all the uncharged particles resulting from first interactions by the primaries, plus the x-rays and annihilation γ-rays emitted by secondary charged particles that are generated by primaries in the attenuator. Multiple scattering is excluded from this ideal case.

3.4.3 Types of geometries and attenuations

The different types of geometries and attenuations can be summarized as follows:

a.) *Narrow-beam geometry*: only primaries strike the detector; μ is observed for monoenergetic beams.

b.) *Narrow-beam attenuation*: only primaries are counted in N_x by the detector, regardless of whether secondaries strike it; μ is observed for monoenergetic beams.